Smart Structures and Systems, Vol. 10, No. 2 (2012) 131-154
DOI: http://dx.doi.org/10.12989/sss.2012.10.2.131

Seismic safety assessment of eynel highway steel bridge using ambient vibration measurements

Ahmet Can Altunişik[1], Alemdar Bayraktar*[1] and Hasan Özdemir[2]

[1]*Karadeniz Technical University, Department of Civil Engineering, 61080, Trabzon, Turkey*
[2]*Prokon Engineering and Consultancy Inc., 29000, Ankara, Turkey*

(Received February 29, 2012, Revised June 2, 2012, Accepted June 21, 2012)

Abstract. In this paper, it is aimed to determine the seismic behaviour of highway bridges by nondestructive testing using ambient vibration measurements. Eynel Highway Bridge which has arch type structural system with a total length of 216 m and located in the Ayvacık county of Samsun, Turkey is selected as an application. The bridge connects the villages which are separated with Suat Uğurlu Dam Lake. A three dimensional finite element model is first established for a highway bridge using project drawings and an analytical modal analysis is then performed to generate natural frequencies and mode shapes in the three orthogonal directions. The ambient vibration measurements are carried out on the bridge deck under natural excitation such as traffic, human walking and wind loads using Operational Modal Analysis. Sensitive seismic accelerometers are used to collect signals obtained from the experimental tests. To obtain experimental dynamic characteristics, two output-only system identification techniques are employed namely, Enhanced Frequency Domain Decomposition technique in the frequency domain and Stochastic Subspace Identification technique in time domain. Analytical and experimental dynamic characteristic are compared with each other and finite element model of the bridge is updated by changing of boundary conditions to reduce the differences between the results. It is demonstrated that the ambient vibration measurements are enough to identify the most significant modes of highway bridges. After finite element model updating, maximum differences between the natural frequencies are reduced averagely from 23% to 3%. The updated finite element model reflects the dynamic characteristics of the bridge better, and it can be used to predict the dynamic response under complex external forces. It is also helpful for further damage identification and health condition monitoring. Analytical model of the bridge before and after model updating is analyzed using 1992 Erzincan earthquake record to determine the seismic behaviour. It can be seen from the analysis results that displacements increase by the height of bridge columns and along to middle point of the deck and main arches. Bending moments have an increasing trend along to first and last 50 m and have a decreasing trend long to the middle of the main arches.

Keywords: ambient vibration measurements; arch type steel highway bridge; dynamic characteristic; enhanced frequency domain decomposition; finite element model updating; nondestructive testing; operational modal analysis; stochastic subspace identification; seismic response

1. Introduction

Bridges are one of the most important engineering structures which are commonly used for interplant and intercity transportation. According to the General Directorate of Highways data, there

*Corresponding author, Professor, E-mail: alemdar@ktu.edu.tr

are 6447 highway bridges with a total length of 296 km in Turkey (GDH 2011). When the high construction cost and logistical importance are considered, it is emerged that the structural response of the highway bridges under dynamic loads should be determined more accurately. Especially, this point is more important for the countries located in the earthquake zone.

The dynamic characteristics of bridge structures are the basis of structural dynamic response and seismic analysis, and are also an important target of health condition monitoring. It is generally expected that finite element models based on technical design data and engineering judgments can yield reliable simulation for both the static and dynamic behaviour. However, because of modelling uncertainties, these finite element models often cannot predict natural frequencies and mode shapes with the required level of accuracy. This raises the need for verification of the finite element models of bridges after construction (Zivanovic *et al.* 2006, Altunışık *et al*. 2010, Bayraktar *et al*. 2010, Altunışık *et al*. 2011).

The dynamic response of a bridge under dynamic loads, such as wind, earthquake or traffic, is very complex and requires special studies. Use of nondestructive experimental measurement tests is advisable to determine the structural properties at the time of opening and during the life time of the bridge (Setra 2006).

There are two basically different techniques available to experimentally identify the dynamic system parameters of a structure: Experimental Modal Analysis and Operational Modal Analysis. In the Experimental Modal Analysis, the structure is excited by known input force and response of the structure is measured. In the Operational Modal Analysis, the structure is excited by unknown input force (ambient vibrations such as traffic load, wind and wave) and response of the structure is measured. Ambient excitations such as traffic, wave, wind, earthquake and their combination are environmental or natural excitations. Therefore, the system identification techniques through ambient vibration measurements become very attractive (Roeck *et al.* 2000).

The Operational Modal Analysis results provide a control mechanism to check the finite element results. If there are differences between analytical and experimental results, the drawbacks in the analytical model can be found and the initial finite element model can be calibrated. This procedure is called as finite element model updating, and can be considered as an attempt to use the best features from both the analytical and experimental models (Bayraktar *et al.* 2011).

In the literature, there were some researches on finite element analysis and nondestructive experimental measurement tests of highway bridges. Feng *et al.* (2004) studied on finite element mode updating of highway bridges by experimental measurement tests data using artificial neural networks. Kwasniewski *et al.* (2006) performed the static and dynamic experimental tests on reinforced concrete highway bridges to determine the dynamic effects, experimentally. Some fully loaded trucks were used as input forces and the response of bridge were collected with the help of accelerometers and displacement transducers. Liu *et al*. (2009) presented a study related to finite element analysis, nondestructive experimental measurements and earthquake behaviour of a three span highway bridges. Whelan *et al.* (2009) deployed a large-scale wireless sensor network for ambient vibration testing of a single-span integral abutment bridge to derive in-service dynamic characteristics. Structural behaviour was measured from ambient and traffic loads with accelerometers to determine the natural frequencies, damping ratios, and mode shapes. Bayraktar *et al.* (2010) determined the dynamic characteristics of Kömürhan Highway Bridge located on Elazığ-Malatya highway in Turkey using finite element analyses and ambient vibration tests. The finite element model of the bridge is updated by changing of some uncertain parameters such as material properties and boundary conditions to eliminate the differences between analytical and experimental dynamic characteristics. Picozzi *et al.* (2010) obtained the structural response of Fatih Sultan Mehmet Bridge, across the Bosporus strait in Istanbul, using wireless monitoring system. Altunışık *et al*. (2011) updated the finite element model of Gülburnu Highway Bridge, constructed with balanced cantilever method, to reflect the current behaviour of the bridge using nondestructive experimental measurement test data. However, there is no enough studies about the finite element analysis, experimental measurements, finite element model updating and seismic safety assessment of arch type steel highway bridges.

This paper describes an arch type steel highway bridge, its analytical modelling, nondestructive experimental measurement tests, finite element model updating using boundary conditions and seismic safety assessment. Eynel Highway Bridge located in Ayvacık county of Samsun, Turkey is selected as an application. Finite element analysis is carried out to extract the analytical dynamic characteristics. Experimental measurements are conducted by ambient vibration tests under traffic, human walking and wind loads; and experimental dynamic characteristics are extracted using Enhanced Frequency Domain Decomposition (EFDD) and Stochastic Subspace Identification (SSI) techniques. Finite element model of the bridge is updated by changing of boundary conditions to reduce the differences between the results. Seismic safety assessment of the bridge before and after model updating is determined using Erzincan earthquake records.

2. Formulation the OMA techniques

Ambient excitation does not lend itself to Frequency Response Function (FRFs) or Impulse Response Function (IRFs) calculations because the input force is not measured in an ambient vibration test. Therefore, a modal identification procedure will need to base itself on output-only data (Ren *et al.* 2004). There are several modal parameter identification methods available. These methods are developed by improvements in computing capacity and signal processing procedures. In this study, two different methods, which are Enhanced Frequency Domain Decomposition (EFDD) in the frequency domain and Stochastic Subspace Identification (SSI) in the time domain, are used for modal parameter extraction.

2.1 Enhanced frequency decomposition domain technique

EFDD technique is an extension to FDD technique which is a basic technique that is extremely easy to use. In the technique, modes are simply picked locating the peaks in Singular Value Decomposition plots (SVD) calculated from the spectral density spectra of the responses. As FDD technique is based on using a single frequency line from the Fast Fourier Transform analysis (FFT), the accuracy of the estimated natural frequency depends on the FFT resolution and no modal damping is calculated. However, EFDD gives an improved estimate of both the natural frequencies and the mode shapes and also includes damping (Jacobsen *et al.* 2006).

In EFDD, the single degree of freedom (SDOF) Power Spectral Density (PSD) function, identified around a peak of resonance, is taken back to the time domain using the Inverse Discrete Fourier Transform (IDFT). The natural frequency is obtained by determining the number of zero-crossing as a function of time, and the damping by the logarithmic decrement of the corresponding SDOF normalized auto correlation function (Jacobsen *et al.* 2006). In FDD technique, the relationship between the unknown input and the measured responses can be expressed as (Bendat and Piersol 2004, Rainieri *et al.* 2007)

$$[G_{yy}(j\omega)] = [H(j\omega)]^{*}[G_{xx}(j\omega)][H(j\omega)]^{T} \tag{1}$$

where $G_{xx}(jw)$ is the rxr Power Spectral Density (PSD) matrix of the input, r is the number of inputs, $G_{yy}(jw)$ is the mxm PSD matrix of the responses, m is the number of responses, $H(jw)$ is the mxr Frequency Response Function (FRF) matrix, and * and superscript T denote complex conjugate and transpose, respectively (Brincker *et al.* 2000).

The FRF can be written in partial fraction, i.e., pole/residue form

$$H(jw) = \sum_{k=1}^{n} \frac{R_k}{jw-\lambda_k} + \frac{R_k^*}{jw-\lambda_k^*} \tag{2}$$

where n is the number of modes λ_k is the pole and, R_k is the residue. Then Eq. (1) becomes as (Brincker *et al.* 2000)

$$G_{yy}(jw) = \sum_{k=1}^{n}\sum_{s=1}^{n}\left[\frac{R_k}{jw-\lambda_k} + \frac{R_k^*}{jw-\lambda_k^*}\right][G_{xx}(jw)]\left[\frac{R_s}{jw-\lambda_s} + \frac{R_s^*}{jw-\lambda_s^*}\right]^{H} \tag{3}$$

where s is the singular values, superscript H denotes complex conjugate and transpose. Multiplying the two partial fraction factors and making use of the Heaviside partial fraction theorem, after some mathematical manipulations, the output PSD can be reduced to a pole/residue form as fallows (Brincker *et al.* 2000)

$$G_{yy}(jw) = \sum_{k=1}^{n} \frac{A_k}{jw-\lambda_k} + \frac{A_k^*}{jw-\lambda_k^*} + \frac{B_k}{-jw-\lambda_k} + \frac{B_k^*}{-jw-\lambda_k^*} \tag{4}$$

where A_k is the k^{th} residue matrix of the output PSD. In the EFDD identification, the first step is to estimate the power spectral density matrix. The estimate of the output PSD $\hat{G}_{yy}(jw)$ known at discrete frequencies $w = w_i$ is then decomposed by taking the SVD of the matrix (Brincker *et al.* 2000)

$$G_{yy}(jw) = U_i S_i U_i^H \tag{5}$$

where the matrix $U_i = [u_{i1}, u_{i2},..., u_{im}]$ is a unitary matrix holding the singular vectors u_{ij}, and S_i is a diagonal matrix holding the scalar singular values s_{ij}. Thus, in this case, the first singular vector u_{ij} is an estimate of the mode shape (Brincker *et al.* 2000). PSD function is identified around the peak by comparing the mode shape estimate u_{ij} with the singular vectors for the frequency lines around the peak. As long as a singular vector is found that has high Modal Assurance Criterion (MAC) value with u_{ij} the corresponding singular value belongs to the SDOF density function (Brincker *et al.* 2000).

From the piece of the SDOF density function obtained around the peak of the PSD, the natural frequency and the damping can be obtained. The piece of the SDOF PSD are taken back to time domain by inverse FFT, and the frequency and the damping is simply estimated from the crossing times and the logarithmic decrement of the corresponding SDOF auto correlation function (Brincker *et al.* 2000).

In the case two modes are dominating the first singular vector will always be a good estimate of the mode shape of the strongest mode. However, in case the two modes are orthogonal, the first singular vectors are unbiased estimates of the corresponding mode shape vectors (Brincker *et al.* 2000).

2.2 Stochastic subspace identification technique

Stochastic Subspace Identification is an output-only time domain method that directly works with time data, without the need to convert them to correlations or spectra. The method is especially suitable for operational modal parameter identification, but it is an incredibly difficult procedure to explain in detail in a short way for civil engineers (Van Overschee and De Moor 1996, Peeters and De Roeck 1999, Peeters 2000). The model of vibration structures can be defined by a set of linear, constant coefficient and second-order differential equations (Peeters and De Roeck 1999)

$$M\ddot{U}(t) + C_*\dot{U}(t) + KU(t) = F(t) = B_*u(t) \tag{6}$$

where M, C_*, K are the mass, damping and stiffness matrices, $F(t)$ is the excitation force, and $U(t)$ is the displacement vector at continuous time t. Observe that the force vector $F(t)$ is factorized into a matrix B_* describing the inputs in space and a vector $u(t)$. Although Eq. (6) represents quite closely the true behavior of a vibrating structure, it is not directly used in SSI methods. So, the equation of dynamic equilibrium (6) will be converted to a more suitable form: the discrete-time stochastic state-space model (Peeters and De Roeck 1999). The state-space model originates from control theory, but it also appears in mechanical/civil engineering to compute the modal parameters of a dynamic structure with a general viscous damping model (Ewins 1984). With the following definitions

$$x(t) = \begin{pmatrix} U(t) \\ \dot{U}(t) \end{pmatrix}, \quad A = \begin{pmatrix} 0 & I_{n_2} \\ -M^{-1}K & -M^{-1}C_* \end{pmatrix}, \quad B = \begin{pmatrix} 0 \\ M^{-1}B_* \end{pmatrix} \tag{7}$$

Eq. (7) can be transformed into the state equation

$$\dot{x}(t) = A\,x(t) + B\,u(t) \tag{8}$$

where A is the state matrix, B is the input matrix and $x(t)$ is the state vector. The number of elements of the state-space vector is the number of independent variables needed to describe the state of a system.

If it is assumed that the measurements are evaluated at only one sensor locations, and that these sensors can be accelerometers, velocity or displacement transducers, the observation equation is (Juang 1994)

$$y(t) = Cx(t) + Du(t) \tag{9}$$

where C is the output matrix and D is the direct transmission matrix. Eqs. (8) and (9) constitute a continuous-time deterministic state-space model. Continuous time means that the expressions can be evaluated at each time instant $t \in \mathbb{N}$ and deterministic means that the input-output quantities $u(t)$, $y(t)$

can be measured exactly. Of course, this is not realistic: measurements are available at discrete time instants $k\Delta t$, $t \in \mathbb{N}$ with Δt, the sample time and noise is always influencing the data. After sampling, the state-space model looks like (Peeters 2000)

$$\left.\begin{aligned} x_{k+1} &= Ax_k + Bu_k \\ y_k &= Cx_k + Du_k \end{aligned}\right\} \tag{12}$$

where $x_k = x(k\Delta t)$ is the discrete-time state vector. The stochastic components (noise) are included and obtained the following discrete-time combined deterministic-stochastic state-space model

$$\left.\begin{aligned} x_{k+1} &= Ax_k + Bu_k + w_k \\ y_k &= Cx_k + Du_k + v_k \end{aligned}\right\} \tag{13}$$

where w_k is the process noise due to disturbances and modeling inaccuracies and v_k is the measurement noise due to sensor inaccuracy. They are both immeasurable vector signals but we assume that they are zero mean, white and with covariance matrices (Peeters 2000)

$$E\left[\begin{pmatrix} w_p \\ v_p \end{pmatrix} \begin{pmatrix} w_q^T & v_q^T \end{pmatrix}\right] = \begin{pmatrix} Q & S \\ S^T & R \end{pmatrix} \delta_{pq} \tag{14}$$

where E is the expected value operator and δ_{pq} is the Kronecker delta. The vibration information that is available in structural health monitoring is usually the responses of a structure excited by the operational inputs that are some immeasurable inputs. Due to the lack of input information it is impossible to distinguish deterministic input u_k from the noise terms w_k, v_k in eq. (13). If the deterministic input term u_k is modeled by the noise terms w_k, v_k the discrete-time purely stochastic state-space model of a vibration structure is obtained (Yu and Ren 2005):

$$\left.\begin{aligned} x_{k+1} &= Ax_k + w_k \\ y_k &= Cx_k + v_k \end{aligned}\right\} \tag{15}$$

Eq. (15) constitutes the basis for the time-domain system identification through operational vibration measurements. The SSI method identifies the state-space matrices based on the output only measurements and by using robust numerical techniques.

2.3 Modal assurance criteria (MAC)

The Modal Assurance Criteria (MAC) is defined as a scalar constant relating the degree of consistency (linearity) between one modal and another reference modal vector (Allemang 2003) as follows,

$$MAC = \frac{\left|\{\phi_{ai}\}^T\{\phi_{ej}\}\right|^2}{\{\phi_{ai}\}^T\{\phi_{ai}\}\{\phi_{ej}\}^T\{\phi_{ej}\}} \tag{16}$$

where $\{\phi_{ai}\}$ and $\{\phi_{ej}\}$ are the modal vectors of i^{th} and j^{th} for different techniques, respectively.

3. Description of the arch type steel highway bridge

Eynel Bridge was selected for the application example in this paper. The investigated arch type steel highway bridge is located in Black Sea region of Turkey, and has a main arch span of 186 m. It connects to the villages near two sides of Suat Uğurlu Dam reservoir in city of Samsun. This bridge was originally designed and constructed by Prokon Engineering and Consultancy, Inc. (Prokon 2011). The construction of the bridge started in 2007 and it was opened to traffic in 2009. Fig. 1 shows some views of the Eynel Highway Bridge.

The bridge is upper-deck steel bridge which has arch type carriage system with a total length of 216 m. The structural system of the bridge consists of the steel arch ribs, vertical and lateral load carrying systems, columns, and the deck system. The span of arch rib is 186 m and it has box-type section. The height and width of the section is 2.4 m and 12 m, respectively. 12 vertical columns (6 on one side) transmit loads from the deck to the arch ribs. The deck is 12 m wide and 10 cm constant thickness. Along its whole length, the arch ribs and deck are stiffened by horizontal brace members. General arrangement drawing of the entire bridge is shown in Fig. 2.

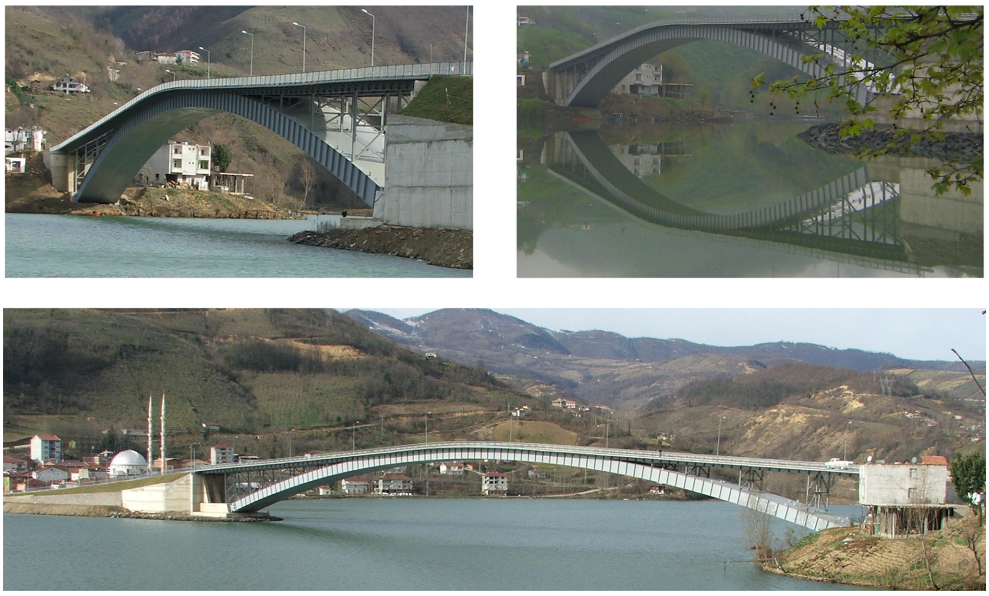

Fig. 1 Some views of Eynel Highway Bridge (Prokon 2011)

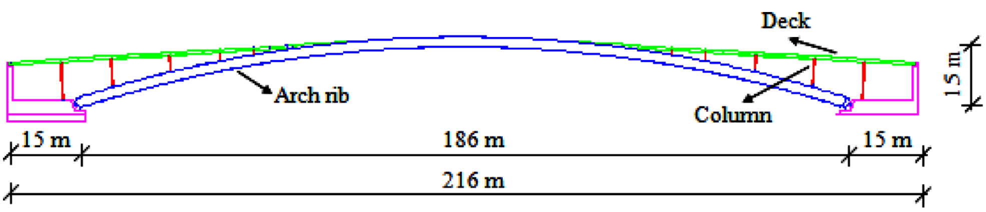

Fig. 2 General arrangement drawing (front view) of the bridge

4. Finite element analysis of eynel highway bridge

Three dimensional finite element model of the Eynel Highway Bridge was constructed using the SAP2000 software (2008). The curve, which defines the axis of the arch, is designed in accordance with the form referred to as the chain curve. In this way, the occurrence of the moment is restricted under the dead load. Also, it is aimed that the arch structural system carries the axial forces.

The selected highway bridge is modelled as a space frame structure with 3D prismatic beam elements which have two end nodes and each end node has six degrees of freedom: three translations along the global axes and three rotations about its axes. The key modelling assumptions are as follows:

- The arch is represented by only one line of elements. The interaction between arch and columns are ensured using rigid body options. The intended number of nodal point displacements can be connected using this option.
- In the finite element model of the bridge, beside the main structural elements fictitious elements are used to determine the torsional and moment effects which consist of asymmetrical load cases according to the bridge axes.
- These elements are defined on the axis through the gravity center of uniform and linear loads.
- These elements are modelled as massless.
- To reflect the rigid diaphragm effect of concrete, diagonal fictitious elements are used on smooth surfaces.
- Fictitious elements are modelled as two ends hinged and one end axial sliding to not act the structural system elements.
- Rigid link elements are modelled as two ends rigid to ensure the torsional moments in the carrier system elements. The elements have high bending rigidity.

To determine the length of the rigid element, it is aimed that fictitious elements are located near the gravity center of the loads. The calculation of the gravity center line is given in Fig. 3. The gravity center line is tried to determine according to the mass distribution. So, the extreme situation on the bridge (full traffic load and full human walking in pedestrian lane) is considered and gravity center line is calculated. Same calculation method about the gravity center line is taken into consideration in the project accountability report. Three dimensional finite element model of Eynel

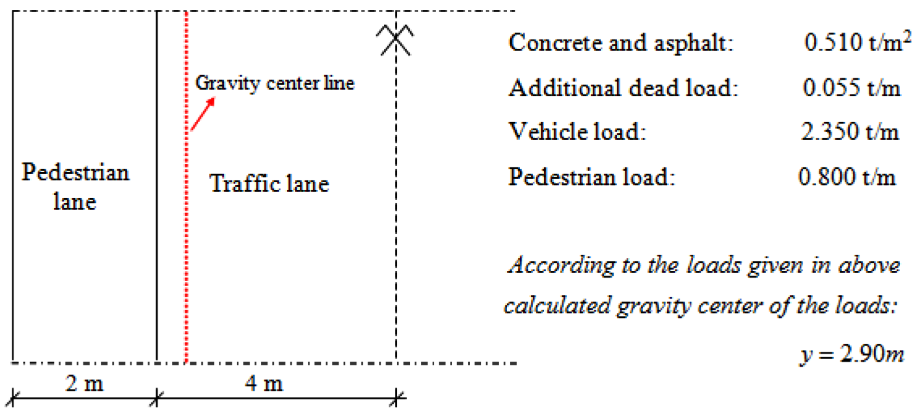

Fig. 3 The calculation of the gravity center line location

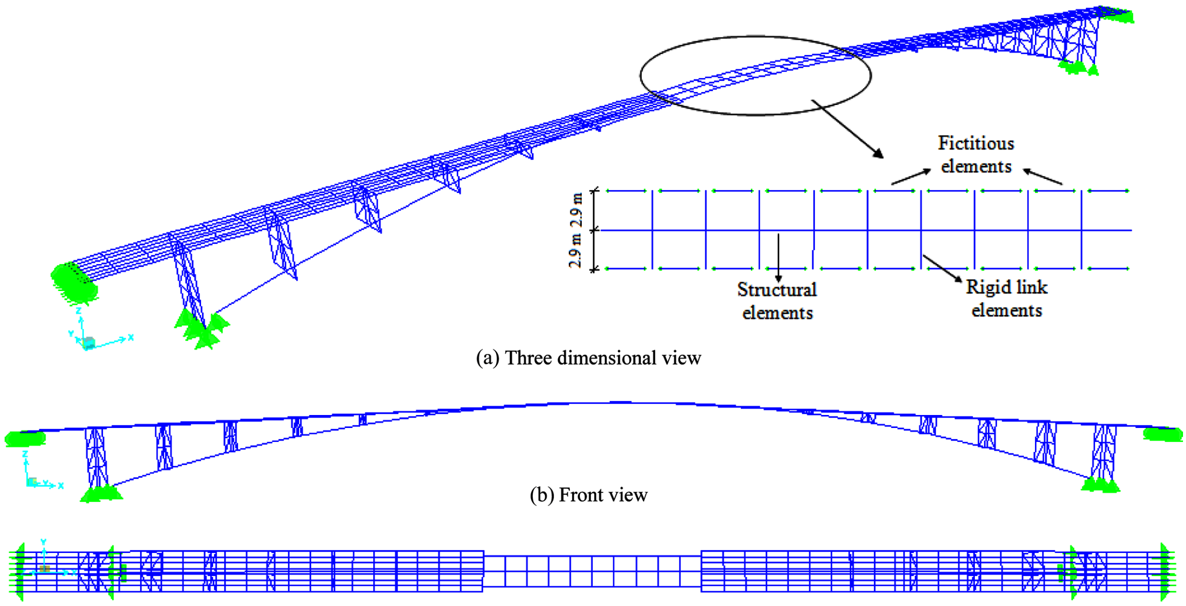

(a) Three dimensional view

(b) Front view

(c) Plan view

Fig. 4 Three dimensional finite element model of Eynel Highway Bridge

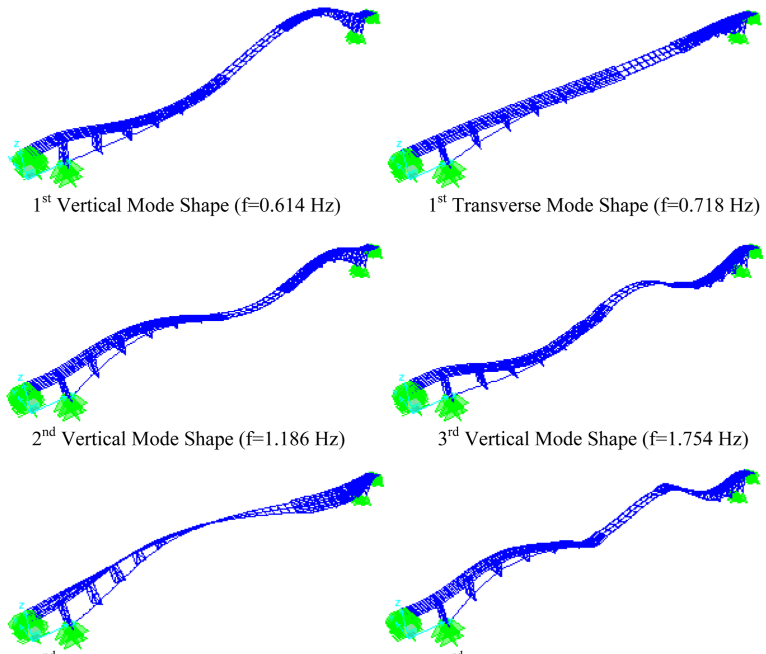

1st Vertical Mode Shape (f=0.614 Hz) 1st Transverse Mode Shape (f=0.718 Hz)

2nd Vertical Mode Shape (f=1.186 Hz) 3rd Vertical Mode Shape (f=1.754 Hz)

2nd Transverse Mode Shape (f=1.940 Hz) 4rd Vertical Mode Shape (f=2.386 Hz)

Fig. 5 Analytically identified the first six mode shapes of the highway bridge

Highway Bridge is given in Fig. 4.

The elastic properties of structural steel were used as material properties in this paper.

Natural frequencies and corresponding vibration modes are important dynamic properties and have significant effect on the dynamic performance of structures. A total of six natural analytical frequencies of the highway bridge are obtained which range between 0.614 and 2.386 Hz. The six analytical vibration modes of the highway bridge as a whole are shown in Fig. 5.

5. Nondestructive measurement tests-operational modal analysis

To determine the dynamic characteristics of engineering structures using experimental measurements, selection of measurement points and measurements setups is very important. Firstly, finite element analysis should be done and dynamic characteristics such as natural frequencies and mode shapes should be obtained, analytically. According to the analytical results, experimental measurement tests properties such as measurement time, frequency span and effective mode number should be determined. Sensitive accelerometer locations should be specified considering analytically determined probable mode points. Because of the fact that data acquisition system has 17-channel, maximum 17 accelerometer locations (measurement points) can be selected in the one measurement test setup. Measurements can be divided into some steps when the intended number of measurements is larger than the number of channels and sensors available. The signals in the substeps are incorporated using a reference accelerometer.

Ambient vibration tests were performed to determine the natural frequencies, mode shapes and damping ratios of Eynel Highway Bridge. For the ambient vibration tests, a B&K 3560 data acquisition system and B&K 8340 type uni-axial seismic accelerometers were used. These accelerometers have 10V/g sensitivity and 0.1-1500 Hz frequency span. During the tests, frequency span was selected as 0-6.25 Hz. The measurements were performed for ten minutes, and excitations were provided from natural effects such as traffic, human walking and wind loads. Signals obtained from the tests were recorded and processed by the commercial software PULSE (2006) and OMA (2006). The dynamic characteristics of the bridge were extracted by EFDD and SSI techniques. Ambient vibration tests were performed using two test setups on the bridge.

· In the first test, seven accelerometers were placed along the center line of the deck in pairs, measuring vertical and transverse accelerations (Fig. 6(a)).
· In the second test setup, 15 accelerometers were used. One of the accelerometers was used as the reference. In addition to the first test, the accelerometers were placed on the two sides of the bridge deck (Fig. 6(b)).

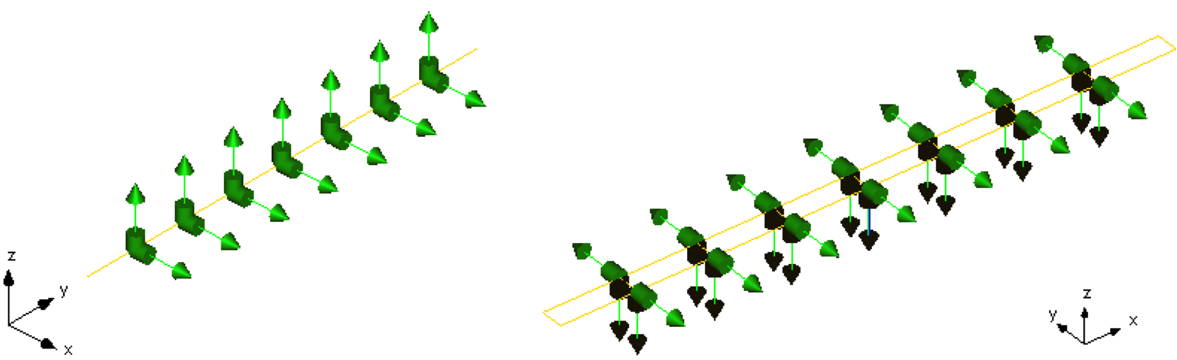

(a) Location of accelerometers in the first test (b) Location of accelerometers in the second test

Fig. 6 Accelerometers locations on the bridge deck during ambient vibration testing

Fig. 7 Some photographs related to ambient vibration tests

Some photographs from the tests appear in Fig. 7.

5.1 Enhanced frequency domain decomposition (EFDD) results

Singular Values of Spectral Density Matrices (SVSDM) and Average of Auto Spectral Densities (AASD) of data set are shown in Figs. 8 and 9 for the first and second tests, respectively. SVSDM are shown in Figs. 8(a) and 9(a) for the first and second tests, respectively. In the first measurement

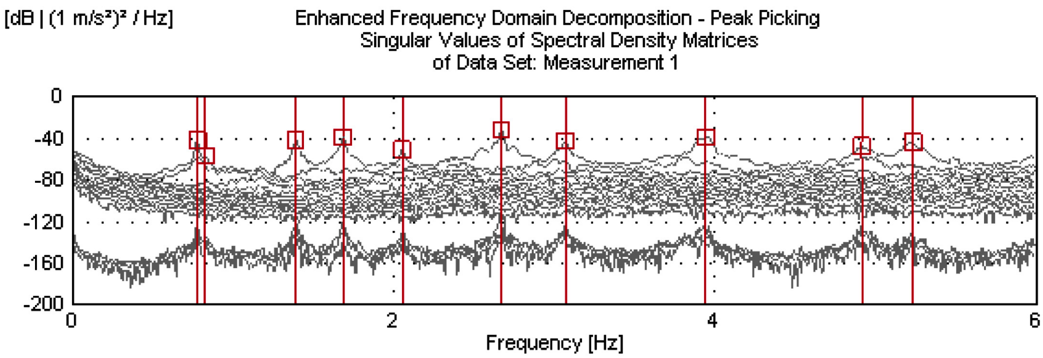

(a) SVSDM of data set

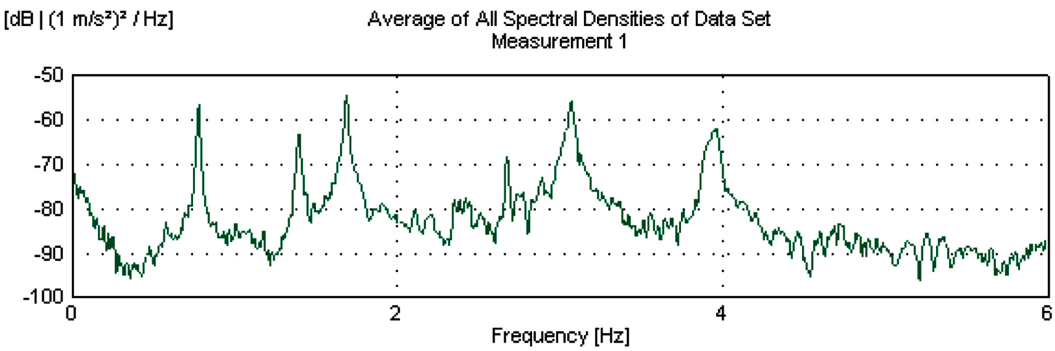

(b) AASD of data set

Fig. 8 SVSDM and AASD of data set for the first test

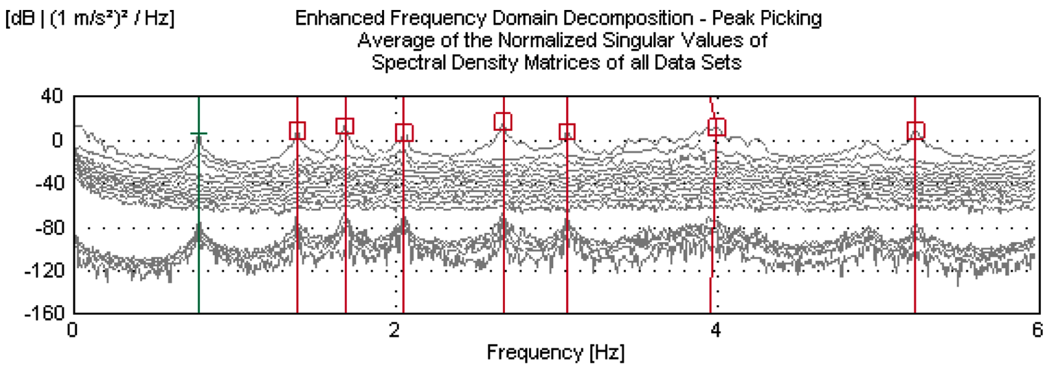

(a) SVSDM of data set

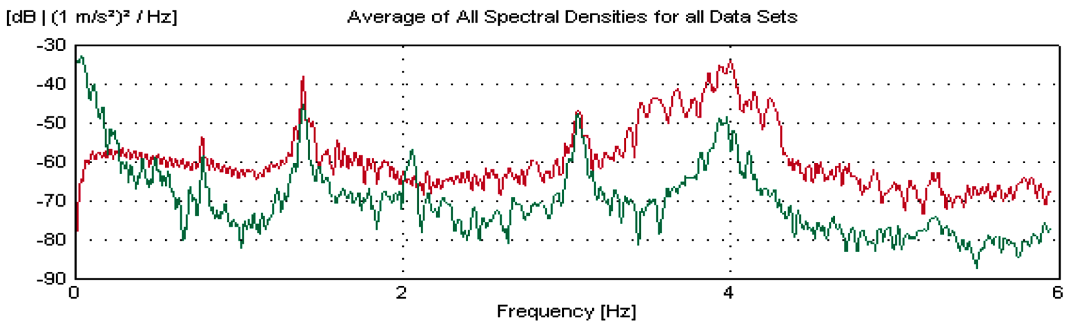

(b) AASD of data set

Fig. 9 SVSDM and AASD of data set for the second test

test a total of 14 accelerometers were placed along to the center line of the deck. After the vibration data analysis using PULSE and OMA software, curves for each accelerometer were obtained (Fig. 8(a)).

Averages of Auto Spectral Densities (AASD) of data set are shown in Figs. 8(b) and 9(b) for the first and second tests, respectively. Because of the fact that intended number of measurements is larger than the number of channels and sensors available, second measurement was divided into two substeps. The signals in the substeps are incorporated using a reference accelerometer. So, two different curves related to first and second substeps are obtained in Fig. 9(b).

The natural frequencies and damping ratios of Eynel Highway Bridge obtained from EFDD technique are listed in Table 1. As seen in Table 1, the first six natural frequencies change between

Table 1 Natural frequencies and damping ratios attained from EFDD technique

Mode	First measurement test		Second measurement test	
	Frequency (Hz)	Damping ratios (%)	Frequency (Hz)	Damping ratios (%)
1	0.779	0.73	0.780	0.82
2	0.828	1.30	-	-
3	1.395	0.51	1.392	0.59
4	1.688	0.40	1.690	0.54
5	2.057	0.45	2.054	1.03
6	2.674	0.25	2.670	0.44

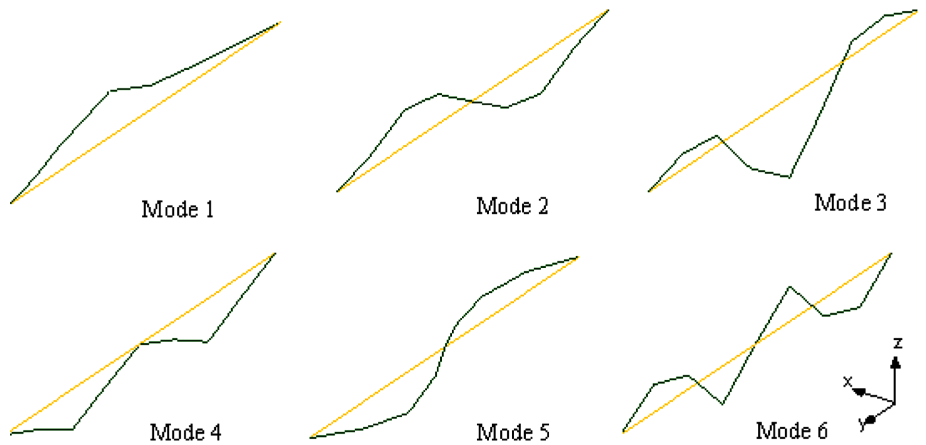

Fig. 10 The mode shapes of the bridge obtained from the first test using EFDD technique

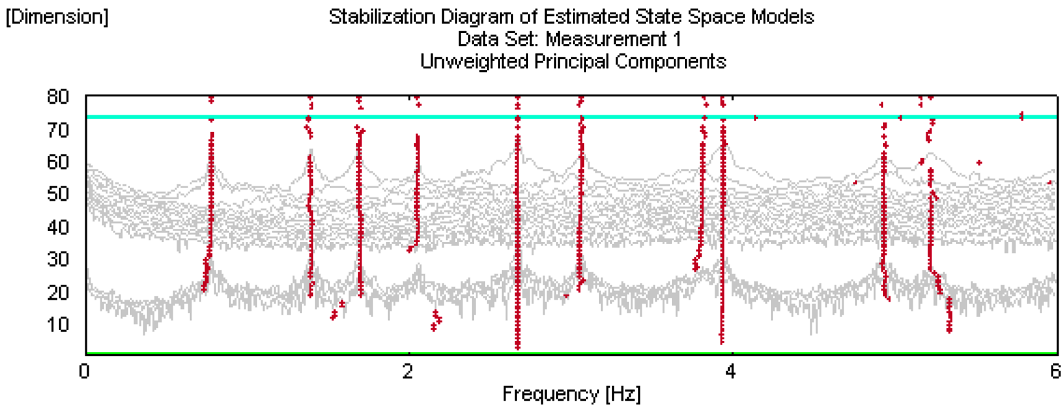

Fig. 11 Stabilization diagram of estimated state space models obtained from the first test

0.779-2.674 Hz. The mode shapes of the bridge obtained from the first and second test setups appear in Fig. 10. As seen in Fig. 10, the mode shapes are vertical and transverse modes.

5.2 Stochastic subspace identification (SSI) results

Stabilization diagrams of estimated state space models for the two tests are given in Figs. 11 and 12, respectively. The natural frequencies and damping ratios obtained from SSI technique are listed in Table 2. As seen in Table 2, the first six natural frequencies change between 0.780-2.670 Hz.

5.3 Comparison of the results

Comparison of natural frequencies obtained from EFDD and SSI techniques for the first and second tests are listed in Table 3. It can be seen from Table 3 that there is a good agreement between EFDD and SSI results. Second mode shapes and its natural frequencies can be extracted from first measurements using EFDD method. But this mode cannot be extracted from first measurements using SSI method and second measurements using EFDD and SSI methods.

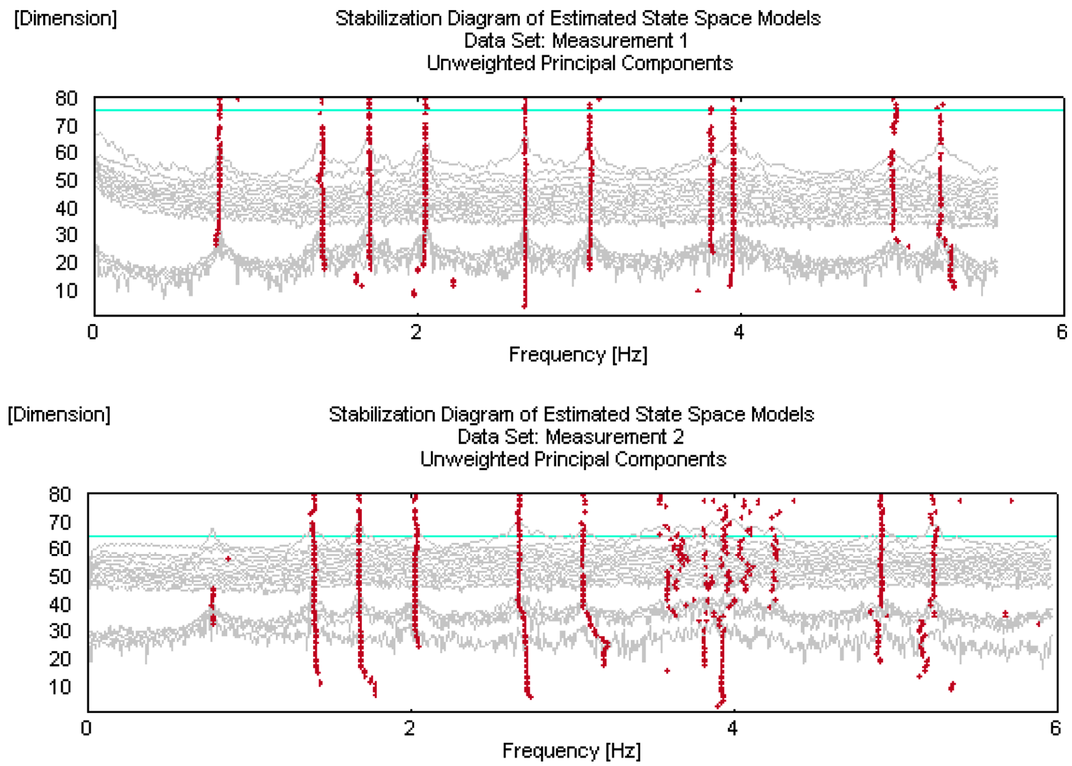

Fig. 12 Stabilization diagram of estimated state space models obtained from the second test

Table 2 Natural frequencies and damping ratios attained from SSI technique

Mode	First measurement test		Second measurement test	
	Frequency (Hz)	Damping ratios (%)	Frequency (Hz)	Damping ratios (%)
1	0.800	1.67	0.780	0.82
2	-	-	-	-
3	1.381	1.06	1.392	0.59
4	1.709	3.26	1.690	0.54
5	1.933	0.84	2.054	1.03
6	2.670	0.36	2.670	0.44

Graphical representations of Modal Assurance Criteria (MAC) related to the first and second tests are shown in Fig. 13. As seen in Fig. 13 that MAC values are almost 90-100%. This shows that all results are almost overlapped. More information about the Modal Assurance Criteria (MAC) can be found in the literature (Allemang 2003, Heylen *et al.* 2007).

When Tables 2 and 3 are examined, it can be seen that the damping ratios are obtained averaged 0.25-3.26% for both measurement tests. These values are compatible with the literature. Comparison of the natural frequencies obtained from finite element analysis and experimental measurements using EFDD and SSI techniques are given in Table 4. It can be seen from Table 4 that there are some differences between analytical and experimental natural frequencies, and experimental natural frequencies are generally bigger than the analytical results. Also, analytically and experimentally

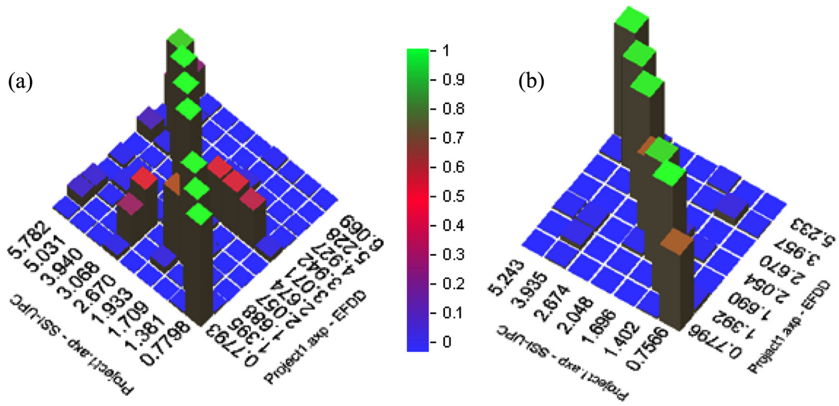

Fig. 13 MAC values for (a) first test and (b) second test

Table 3 Comparison of the natural frequencies obtained from EFDD and SSI techniques

Mode	First measurement test				Second measurement test			
	EFDD (Hz)	SSI (Hz)	Diff. %	MAC	EFDD (Hz)	SSI (Hz)	Diff. %	MAC
1	0.779	0.800	2.63	0.998	0.780	0.757	2.95	0.669
2	0.828	-	-	-	-	-	-	-
3	1.395	1.381	1.00	0.990	1.392	1.402	0.713	0.999
4	1.688	1.709	1.23	0.989	1.690	1.696	0.354	0.924
5	2.057	1.933	6.03	-	2.054	2.048	0.293	0.660
6	2.674	2.670	0.096	1.000	2.670	2.674	0.150	0.962

Table 4 Comparison of the analytical and experimental natural frequencies

Mode number	Analytical frequencies	First measurement test			Second measurement test		
		EFDD (Hz)	SSI (Hz)	Diff. %	EFDD (Hz)	SSI (Hz)	Diff. %
1	0.614	0.779	0.800	23.25	0.780	0.757	21.28
2	0.718	0.828	-	13.28	-	-	-
3	1.186	1.395	1.381	14.98	1.392	1.402	15.41
4	1.754	1.688	1.709	4.22	1.690	1.696	3.65
5	1.940	2.057	1.933	5.69	2.054	2.048	5.55
6	2.386	2.674	2.670	10.77	2.670	2.674	10.77

identified first mode shapes are different. So, it is thought that initial finite element model of the bridge must be updated using some uncertain parameters according to the nondestructive measurements results to reduce the differences for the seismic safety assessment of the bridge.

6. Finite element model updating of the bridge

In modern analysis of structures, much effort is devoted to the derivation of accurate models. These accurate models are used in many applications of civil engineering structures like damage detection, health monitoring, structural control, structural evaluation, and assessment. In the development of finite element models of structures, it is usual to make simplifying assumptions. The finite element model of a structure is constructed on the basis of highly idealized engineering blueprints and designs that may or may not truly represent all the physical aspects of an actual structure. When field tests are performed to validate the analytical model commonly natural frequencies and mode shapes, do not coincide with the expected results from the analytical model. These discrepancies originate from the uncertainties in simplifying assumptions of structural geometry, materials, as well as inaccurate boundary conditions. The problem of how to modify the analytical model from the dynamic measurements is known as the model updating in structural dynamics (Jaishi and Ren 2005). The main purpose of the model updating procedure is to minimize the differences between the analytically and experimentally obtained dynamic characteristics by changing of some uncertainty parameters such as material properties and boundary conditions.

The updating process typically consists of manual tuning and then automatic model updating using some specialised software. The manual tuning involves manual changes of the model geometry and modelling parameters by trial and error, guided by engineering judgement. The aim of this is to bring the numerical model closer to the experimental one (Zivanovic *et al.* 2007). In this study, the manual tuning procedure is used for finite element model updating.

When the analytically and experimentally identified dynamic characteristics of Eynel Highway Bridge are compared with each other, there are some differences between analytical and experimental natural frequencies, and experimental natural frequencies are generally bigger than the other. Also, analytically and experimentally identified first mode shapes are different. It is thought that these differences resulted from some uncertainties in the structural geometry, material properties and boundary conditions accepted in the design phase of the bridge.

6.1 Updating of the material properties

Because of the fact that the raw material of structural geometry of the bridge is steel, the material properties are not chosen as updating parameters.

6.2 Updating of the boundary condition

In the initial finite element model of the bridge, selected boundary conditions related to the node numbers at the left side of the bridge (Fig. 14) is summarized in Table 5. For the deck-type arch

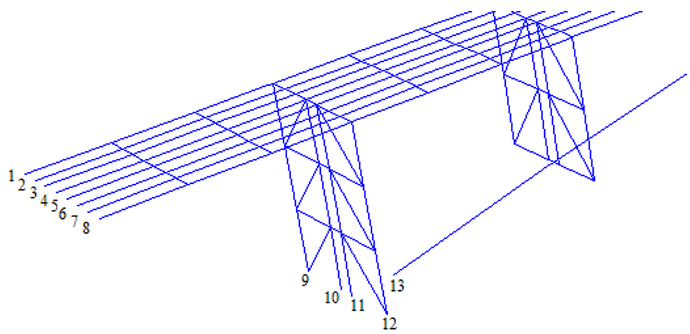

Fig. 14 The left side view of the bridge including node numbers

Table 5 Boundary conditions related to the node numbers

Node number	Restraints					
	X	*Y*	*Z*	*RX*	*RY*	*RZ*
1	No	Yes	Yes	No	No	No
2	No	Yes	Yes	No	No	No
3	No	Yes	Yes	No	No	No
4	No	Yes	Yes	No	No	No
5	No	Yes	Yes	No	No	No
6	No	Yes	Yes	No	No	No
7	No	Yes	Yes	No	No	No
8	No	Yes	Yes	No	No	No
9	Yes	Yes	Yes	No	No	No
10	Yes	Yes	Yes	No	No	No
11	Yes	Yes	Yes	No	No	No
12	Yes	Yes	Yes	No	No	No
13	Yes	Yes	Yes	Yes	No	Yes

bridge, the boundary conditions of the side columns connected between the arch and the main girder are fixed in order to transmit the longitudinal load on the deck.

As it is seen from Fig. 14 and Table 5, displacements capacities in all directions (*Ux*, *Uy* and *Uz*) and rotational capacities in some directions (*Rx* and *Rz*) at the corner nodes of main arches are restricted. Only, rotational capacities in one direction (*Ry*) at the corner nodes of main arches are allowed.

In the finite element model updating, semi-rigid connections are considered at this points and rotational capacities in Ry direction are restricted as part of. The joints modelled in the finite element model of the main arches are given in Fig. 15. The corresponding structural element connections to joints are considered as semi-rigid. The values of linear rotational spring stiffness defined at the end of the main arches are determined using the parameters given in Table 6.

In the analysis, structural elements such as main arch, deck and piers divided into finite elements to obtain the more reliable result. The mean of 9.42 m given in Table 6 is the length of first finite

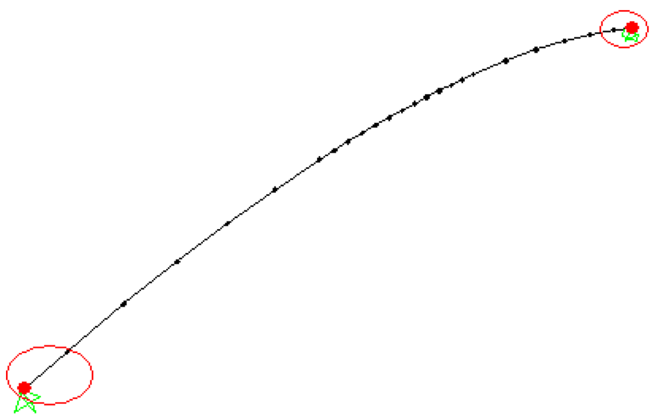

Fig. 15 Connection points on the finite element model of the main arches

Table 6 Rotational spring stiffness values for finite element model updating

Structural element	Modules of elasticity (N/m^2)	Length (m)	Moment of inertia (cm^4)	K_y (Nm/rad)	K_z (Nm/rad)
Main arches	2.062E11	9.42	517E5	1E7	1E7

Table 7 Analytical and experimental dynamic characteristics after model updating

Mode number	Initial finite element model		Measurement tests		Updated finite element model	
	Frequency (Hz)	Max. Diff. (%)	EFDD (Hz)	SSI (Hz)	Frequency (Hz)	Max. Diff. (%)
1	0.614	23.25	0.779	0.800	0.770	3.75
2	0.718	13.28	0.828	-	0.860	3.72
3	1.186	14.98	1.395	1.381	1.488	7.19
4	1.754	4.22	1.688	1.709	1.728	1.10
5	1.940	5.69	2.057	1.933	1.890	2.22
6	2.386	10.77	2.674	2.670	2.690	0.01

elements of main arch.

K_y and K_z given in Table 6 are calculated by using equation given below (Altunışık *et al.* 2010)

$$k_{i,j} = \frac{3EI\nu_{i,j}}{(1-\nu_{i,j})L} \tag{17}$$

where E: modules of elasticity, I: moment of inertia, L: length and $\nu_{i,j}$ connection percentages. The stiffness coefficient $k_{i,j}$ is defined as the force at the nodal coordinate i when a unit displacement is given at the nodal coordinate j (all other nodal coordinate are kept fixed) (Paz and Leigh 2001).

6.3 Updating of the other structural properties

15 kN/m distributed load is added on the bridge deck considering the weight of the 8 cm asphalt, sidewalks and scarecrows.

Comparison of the analytical and experimental dynamic characteristics of the Eynel Highway Bridge before and after finite element model updating is given in Table 7. According to Table 7, it is seen that there is a good agreement between natural frequencies, and maximum differences are reduced averagely from 23% to 3% after finite element model updating.

Comparison of the analytical and experimental mode shapes after finite element model updating is given in Fig. 16. It is seen from Fig. 16 that there is a good harmony between mode shapes after finite element model updating. So, it is thought that updated finite element model reflect the current behaviour of the highway bridge and it can be used to predict the seismic response of the bridge under complex external forces.

7. Seismic behaviour of the bridge

Seismic behaviour of Eynel Highway Bridge before and after finite element model updating is performed using 1992 Erzincan earthquake ground motion (PEER 2011) (Fig. 17). This earthquake has a magnitude value as 6.9 (M=6.9). East-West (ERZ/EW) component of the ground motion are

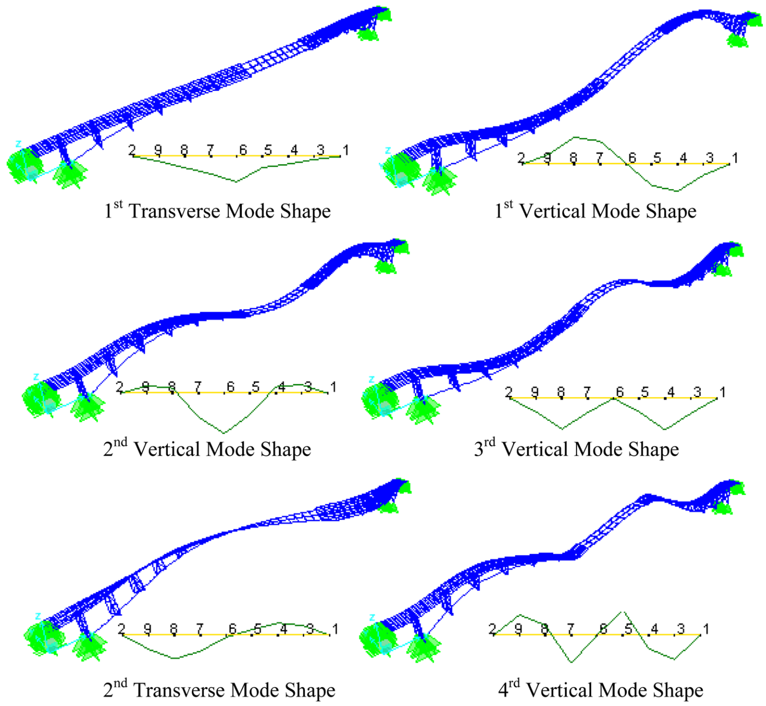

Fig. 16 Comparison of the analytical and experimental mode shapes after model updating

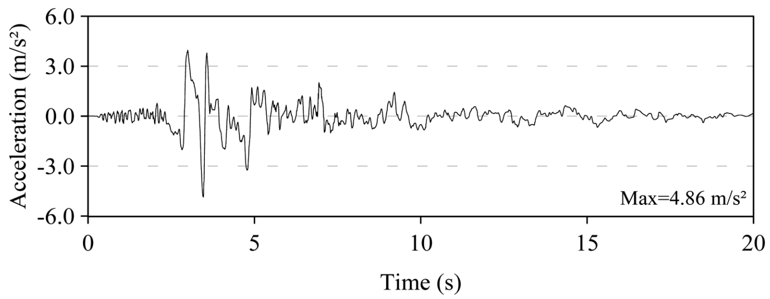

Fig. 17 Time histories of ground motion accelerations of 1992 Erzincan earthquake

applied to the bridge at the vertical direction. In the dynamic analysis, first 6 modes are considered. Also, experimentally identified damping ratios for each mode are considered in the updated analytical finite element model.

7.1 Deck response

Distribution of the vertical displacements along the bridge deck before and after finite element model updating is given in Fig. 18. It is seen from Fig. 18 that displacements after model updating are bigger than the other. Vertical displacements have an increasing trend along to middle of the bridge deck and main arches.

The maximum vertical displacements are obtained as 8.93 cm and 20.20 cm before and after

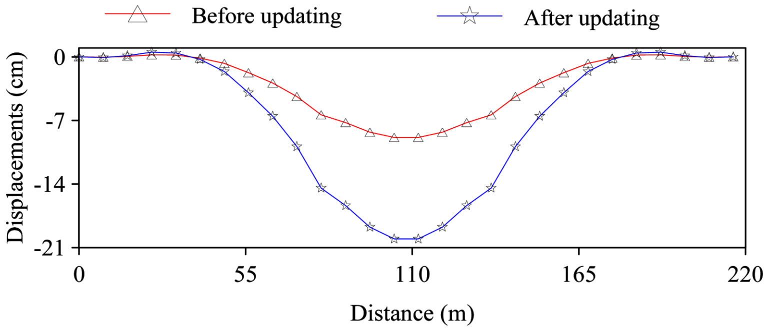

Fig. 18 Changing of maximum displacements along the bridge deck

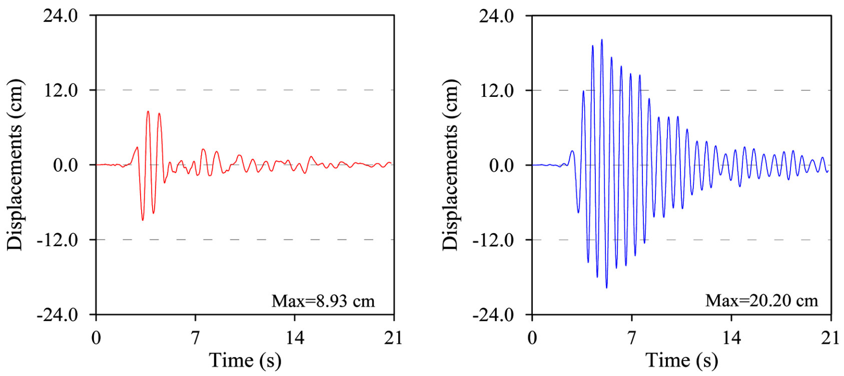

(a) Before model updating (b) After model updating

Fig. 19 Time histories of the maximum vertical displacements for bridge deck

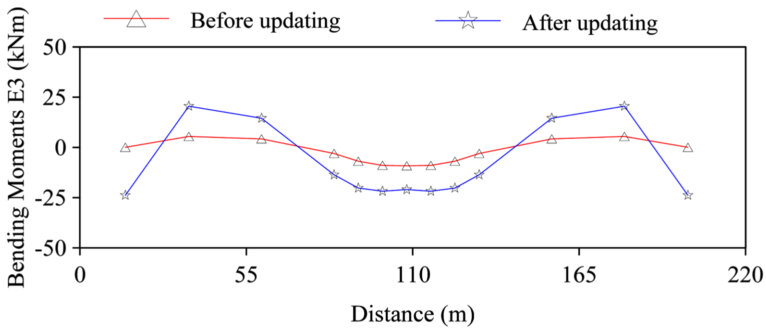

Fig. 20 Changing of maximum bending moments along the main arches

model updating respectively. The time histories of maximum displacements before and after model updating are presented in Fig. 19.

Distribution of the bending moments along the main arches before and after finite element model updating is given in Fig. 20. It is seen from Fig. 20 that the distribution of the bending moments is similar except the corner nodes. Bending moments have an increasing trend along to first and last 50 m and have a decreasing trend long to the middle of the main arches.

The time histories of maximum bending moments before and after model updating occurred as 10.45×10^{3} kNm and 24.05×10^{3} kNm, respectively on the main arches obtained from seismic analysis

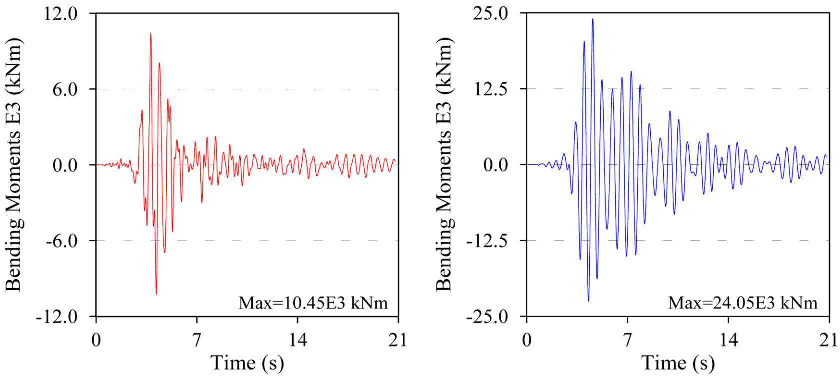

(a) Before model updating (b) After model updating

Fig. 21 Time histories of maximum bending moment for main arches

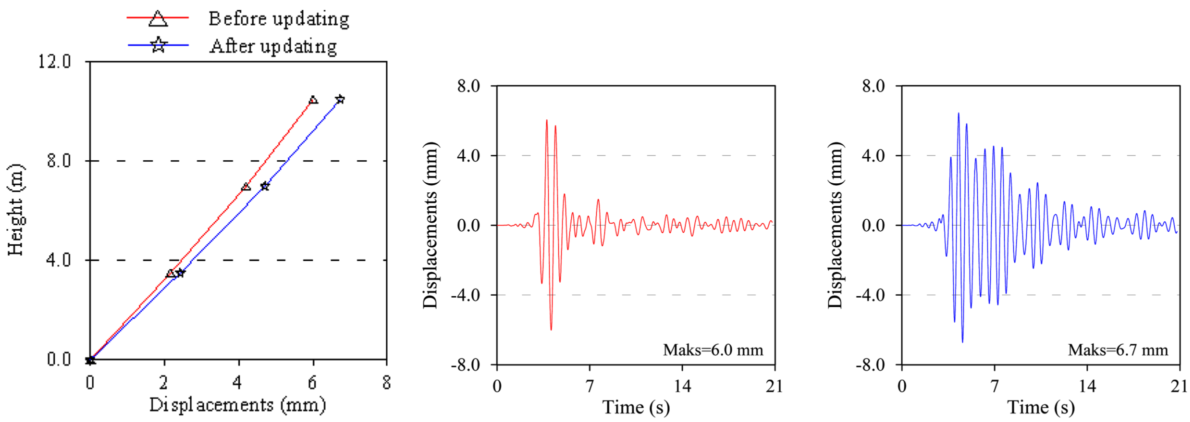

(a) Changing of lateral displacements (b) Before updating (c) After updating

Fig. 22 Changing of lateral displacements along the bridge columns (a) and time histories of maximum lateral displacements before (b) and after (c) modal updating

subjected to Erzincan ground motion is presented in Fig. 21.

7.2 Column response

The variation of lateral displacements along to the height of the bridge column (side columns near the corner node of main arches) and the time histories of maximum displacements before and after finite element model updating are presented in Fig. 22. It can be seen in Fig. 22 that the lateral displacements increase along the height of bridge column.

8. Conclusions

This paper aimed to determine the seismic behaviour of Eynel Highway Bridge by nondestructive testing using ambient vibration measurements. Finite element model of the bridge is conducted and analytical modal analysis is performed to generate natural frequencies and mode shapes. The ambient vibration measurements are carried out on the bridge deck using Operational Modal Analysis. Analytical and experimental dynamic characteristic are compared with each other and finite element model of the bridge is updated by changing of boundary conditions to reduce the differences between the results. Analytical model of the bridge before and after model updating is analyzed using 1992 Erzincan earthquake record to determine the seismic behaviour. The conclusions drawn from the study can be presented as below:

- From the finite element model of the highway bridge, a total of six natural frequencies were attained analytically, which range between 0.614 and 2.386 Hz. Considering the first six mode shapes, these modes can be classified into vertical and transverse modes.
- The experimental natural frequencies and mode shapes obtained from EFDD and SSI techniques for the first and second tests are generally close to each other. The first six natural frequencies are obtained between 0.779-2.674 Hz from both techniques.
- Vertical and transverse mode shapes are obtained for both EFDD and SSI techniques.
- The MAC values for EFDD and SSI results are generally calculated between 90-100%.
- The damping ratios are obtained between 0.25-3.26% for the two tests. The damping ratios obtained from the second tests results for EFDD and SSI are close to each other.
- When the comparing of analytical and experimental results, it was seen that there was an approximate 23% difference between the natural frequencies predicted by the initial finite element model and obtained through Operational Modal Analysis. Experimental frequencies are bigger than those of the analytical. Also, analytically and experimentally identified first mode shapes are different.
- To eliminate differences, finite element model of the bridge was updated by adjusting of boundary conditions. After finite element model updating, maximum differences between the natural frequencies was averagely reduced to 3%.
- Good agreement was found between natural frequencies and mode shapes obtained from updated finite element model of the bridge and experimental results.
- Seismic evaluations of the bridge before and after finite element model updating were determined using 1992 Erzincan earthquake ground motion. EW component of the ground motion is applied to the bridge at the vertical direction. Experimentally identified damping ratios were considered in the updated finite element analyses. It can be seen from the analysis results that displacements increase by the height of bridge columns and along to middle point of the deck and main arches.
- The maximum vertical displacements are obtained as 8.93 cm and 20.20 cm for bridge deck before and after model updating, respectively.
- Distribution of the bending moments along the main arches before and after finite element model updating is given with detail. Bending moments have an increasing trend along to first and last 50 m and have a decreasing trend long to the middle of the main arches. Maximum bending moments occurred as 10.45×10^3 kNm and 24.05×10^3 kNm for main arches before and after model updating, respectively.
- The variation of lateral displacements along to the height of the bridge column and the time histories of maximum displacements before and after finite element model updating are given with detail. It is seen that the lateral displacements increase along the height of bridge column and maximum displacements are obtained as 6.0 mm and 6.7 mm before and after model updating, respectively.
- It is seen that the ambient vibration measurements using EFDD and SSI techniques are enough to identify the most significant modes of steel highway bridges.

Acknowledgements

This research was supported by TUBITAK and Karadeniz Technical University (KTU) under Research Grant No. 106M038 and 2006.112.001.1, respectively. The authors thank to Prokon Engineering and Consultancy Inc. to supply the project data and drawings.

References

Allemang, R.J. (2003), "The modal assurance criterion: twenty years of use and abuse", *J. Sound Vib.*, **37**(8), 14-23.

Altunışık, A.C., Bayraktar, A., Sevim, B. and Ateş, S. (2011), "Ambient vibration based seismic evaluation of isolated gülburnu highway bridge", *Soil Dyn. Earthq. Eng.*, **31**(11), 1496-1510.

Altunışık, A.C., Bayraktar, A., Sevim, B. and Özdemir, H. (2011), "Experimental and analytical system identification of eynel arch type steel highway bridge", *J. Constr. Steel Res.*, **67**(12), 1912-1921.

Altunışık, A.C., Bayraktar, A., Sevim, B., Kartal, M.E. and Adanur, S. (2010), "Finite element model updating of an arch type steel laboratory bridge model using semi-rigid connection", *Steel Compos. Struct.*, **10**(6), 543-563.

Bayraktar, A., Altunışık, A.C., Sevim, B. and Türker, T. (2010), "Earthquake behaviour of kömürhan highway bridge using validated finite element model", *J. Test. Eval.*, **38**(4), 467-481.

Bayraktar, A., Sevim, B. and Altunl ık, A.C. (2011), "Finite element model updating effects on nonlinear seismic response of arch dam-reservoir-foundation systems", *Finite Elemen. Anal. Des.*, **47**(2), 85-97.

Bendat, J.S. and Piersol, A.G. (2004), *Random data: analysis and measurement procedures*, John Wiley and Sons, USA.

Brincker, R., Zhang, L. and Andersen, P. (2000), "Modal identification from ambient responses using frequency domain decomposition", *Proceedings of the 18th International Modal Analysis Conference*, San Antonio, USA.

Ewins, D.J. (1984), *Modal testing: theory and practice*, Letchworth, Hertfordshire, England: Research Studies Press, New York.

Feng, M.Q., Kim, D.K., Yi, J.H. and Chen, Y. (2004), "Baseline models for bridge performance monitoring", *J. Eng. Mech.- ASCE*, **130**(5), 562-569.

GDH. (2011), *General directorate of highways*, Ankara, Turkey.

Heylen, W., Stefan, L. and Sas, P. (2007), *Modal analysis theory and testing*, Katholieke Universiteit Leuven, Faculty of Engineering, Department of Mechanical Engineering, Leuven, Belgium.

Jacobsen, N.J., Andersen, P. and Brincker, R. (2006), "Using enhanced frequency domain decomposition as a robust technique to harmonic excitation in operational modal analysis", *Proceedings of the ISMA2006: International Conference on Noise & Vibration Engineering*, Leuven, Belgium.

Jaishi, B. and Ren, W.X. (2005), "Structural finite element model updating using ambient vibration test results", *J. Struct. Eng. - ASCE*, **131**(4), 617-628.

Juang, J.N. (1994), *Applied system identification*, Englewood Cliffs (NJ): Prentice-Hall Inc.

Kwasniewski, L., Wekezer, J., Roufa, G., Hongyi, L., Ducher, J. and Malachowski, J. (2006), "Experimental evaluation of dynamic effects for a selected highway bridge", *J. Perform. Constr. Fac.*, **20**(3), 253-260.

Liu, C., DeWolf, J.T. and Kim, J.H. (2009), "Development of a baseline for structural health monitoring for a curved post-tensioned concrete box girder bridge", *Eng. Struct.*, **31**(12), 3107-3115.

OMA. (2006), *Operational modal analysis. release 4.0*, Structural Vibration Solutions A/S; Denmark.

Paz, M. and Leigh, W. (2001), *Integrated matrix analysis of structures*, Theory and Computation, Kluwer Academic Publishers, Boston, London.

PEER. (2011), *Pacific earthquake engineering research centre*, http://peer.berkeley.edu/smcat/Peeters, B. (2000), *System identification and damage detection in civil engineering*, PhD Thesis, K.U, Leuven, Belgium.

Peeters, B. and De Roeck, G. (1999), "Reference based stochastic subspace identification in civil engineering", *Proceedings of the 2nd International Conference on Identification in Engineering Systems*, Swansea, UK.

Picozzi, M., Milkereit, C., Zulfikar, C., Fleming, K., Ditommaso, R., Erdik, M., Zschau, J., Fischer, J., Þafak, E., Özel, O. and Apaydýn, N. (2010), “Wireless technologies for the monitoring of strategic civil infrastructures: an ambient vibration tests on the fatih sultan mehmet suspension bridge in istanbul, Turkey”, *Bull. Earthq, Eng*., **8**(3), 671-691.

Prokon. (2011), *Prokon engineering and consultancy Inc*., Ankara, Turkey.

PULSE. (2006), *Labshop*, Version 11.2.2. Bruel and Kjaer, Sound and Vibration Measurement A/S; Denmark.

Rainieri, C., Fabbrocino, G., Cosenza, E. and Manfredi, G. (2007), “Implementation of OMA procedures using labview: theory and application”, *Proceedings of the 2nd International Operational Modal Analysis Conference*, 30 April-2 May, Copenhagen, Denmark, 1-13.

Ren, W.X., Zhao, T. and Harik, I.E. (2004), “Experimental and analytical modal analysis of steel arch bridge”, *J. Struct. Eng. - ASCE*, **130**(7), 1022-1031.

Roeck, G.D., Peeters, B. and Ren, W.X. (2000), “Benchmark study on system identification through ambient vibration measurements”, *Proceedings of the 18th International Modal Analysis Conference*, San Antonio, USA, 1106-1112.

SAP2000. (2008), *Integrated finite element analysis and design of structures*, Computers and Structures Inc., Berkeley, California, USA.

Setra. (2006), *Footbridges Assessment of Vibrational Behaviour of Footbridges under Pedestrian Loading*, Technical Guide Published by the Setra, French Association of Civil Engineering, France.

Van Overschee, P. and De Moor, B. (1996), *Subspace identification for linear systems: theory, implementation and applications*, Kluwer Academic Publishers, Dordrecht, Netherlands.

Whelan, M.J., Gangone, M.V., Janoyan, K.D. and Jha, R. (2009), “Real-time wireless vibration monitoring for operational modal analysis of an integral abutment highway bridge”, *Eng. Struct*., **31**(10), 2224-2235.

Yu, D.J. and Ren, W.X. (2005), “EMD-based stochastic subspace identification of structures from operational vibration measurements”, *Eng. Struct*., **27**(12), 1741-1751.

Zivanovic, S., Pavic, A. and Reynolds, P. (2006), “Modal testing and fe model tuning of a lively footbridge structure”, *Eng. Struct*., **28**(6), 857-868.

Zivanovic, S., Pavic, A. and Reynolds, P. (2007), “Finite element modelling and updating of a lively footbridge: the complete process”, *J. Sound Vib*., **301**(1-2), 126-145.

CC